International Journal of Applied Engineering Research
ISSN 0973-4562 Volume 10, Number 7 (2015) pp. 18395-18406

http://www.ripublication.com

Optimization Analysis of Microwave Ring Resonator for Bio-sensing Application

Rammah A. Alahnomi*[1], Z.Zakaria[2], E.Ruslan[3], A. A. M. Isa[4], A. A. M. Bahar[5]

[1, 2, 4, 5] Center for Telecommunication Research and Innovation (CeTRI), Faculty of Electronics and Computer Engineering, University Technical Malaysia Melaka (UTeM), Hang Tuah Jaya, 76100 Durian Tunggal, Melaka, Malaysia.
[3] Faculty of Technology Engineering (FTK), University Technical Malaysia (UTeM), Hang Tuah Jaya, 76100 Durian Tunggal, Malacca, Malaysia.
*E-Mail: *[1]alrammah89@gmail.com, [2]zahriladha@utem.edu.my*

Abstract

This paper investigates the performance of simple models based on ring resonator techniques for materials characterization. These techniques are used because they are cost effective, simple, and easy to fabricate, easy to simulate, easy to enhance the accuracy of the sensor with respect to material characterization compared to other techniques. Among different techniques, it is required to consider many factors in order to optimize an appropriate method. The structure of 2.2GHz is designed for different types of resonator and then simulated using the CST software simulator. The calculated and simulation results are evaluated by comparing with different types of ring resonators. The most significant of these techniques are to be used for various industrial applications such as food industry, quality control, bio –sensing medicine and pharmacy.

Keywords: CST Simulator, Dielectric Measurement Techniques, Material Characterization, Ring Resonators.

Introduction

Dielectric property is an important field of the material characterization and sensing subjects.Each material has a unique set of electrical characterization which are dependent on the properties of the dielectric. These properties measurements provide

valuable information for scientists in order to properly incorporate the material into its intended application such as monitoring a manufacturing process for improving quality control and testing. Several measurement techniques have been developed for characterizing the dielectric properties of materials [1]-[4].

The microstrip ring resonator is one of these measurement techniques and it is developed from being just a characterization tool to evaluate microstrip parameters, to the realm of circuit application. It exhibits a periodic frequency response with well-known resonance frequencies, that can be exploited to determine material properties and in specific the dielectric constant and line losses [5]-[6]. Recently, microwave technologies play a key role in increasing number of military and industry applications. It is being used in the tunable and switchable filters and oscillators [7]-[9], and microwave circuit including antenna and couplers [10]-[11].

In the microwave resonator design, the permittivity of the dielectric substrate has gained an important role and requires precise evaluation over a broad range of frequencies. The microwave resonator has been modeled in several ways with both field techniques [11]-[12] and circuit techniques [13]. Chang [11] developed an equivalent circuit model for the ring resonator when operates near to the lowest resonant frequency by using transmission line theory. Jilani [12]-[13] studied the microstrip ring resonators based sensor for meat quality and described the modeling of biological tissues using equivalent lumped elements.

There are various kinds of a biosensor on bio-sensing technologies based on fluorescence [14], electromechanical transduction [15], nano-materials [16], and surface resonance Plasmon (SPR) [17]. Even though these bios-sensors are successful and useful, they often required bulky measurement equipment, complex fabrication steps, time consuming for the processes which make the biological analysis system complex and expensive.

In this paper, it presents a structurally simple and direct bio-sensors detection methods. For structural simplicity, it is utilized a microwave ring resonator with two coupling gap and feed lines, ring resonator with one/two slits, stub matched loose ring resonator, and enhanced coupling gap ring resonator whose resonant frequency is 2.2GHz. Findings and analysis of material measurement technique development are discussed for different types of ring resonators and various factors are considered in order to obtain an appropriate technique, which provides high accuracy, low cost, easy procedures, and rapid measurement of the desired testing material. This work concentrates on the Microstrip ring resonator techniques as a method of measuring material properties, which can be used to infer information about the dielectric.

Design Structure

The ring resonator device consists entirely of printed Microstrips on a rigid substrate. A two layer board with one dielectric material is used, as demonstrated in Figure 1. It illustrates the relative positions of the feed lines and ring on the upper surface of the board. The feed lines and ring resonator are printed transmission lines with width chosen for 50 Ωcharacteristic impedance. A small gap (g) is included between the ring and each feed line; this gap is included to separate the resonant behavior of the

ring from the feed network and ranges from 0.1 to 1.0 times the width of the feed Microstrip.

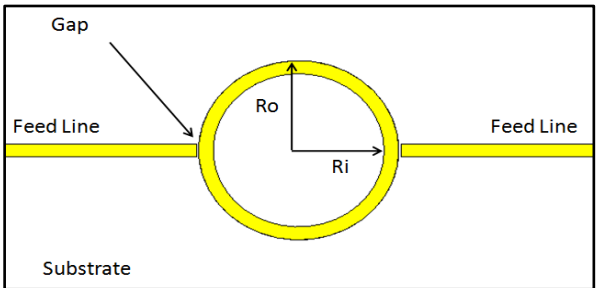

Figure 1: Microwave ring resonator for measurement

For the ring resonator, the resonance is produced when the mean circumference of the ring resonator is equal to an integral of the guided wavelength

$$2\pi r = n\lambda g \quad (1)$$

Where n= 1, 2, 3, 4… and so on.
We can calculate the resonant frequency for n modes by using

$$\lambda g = \frac{\lambda}{\sqrt{\varepsilon eff}} \quad (2)$$

Where:

$$\lambda = \frac{c}{f}$$

So, by considering equations (1) and (2), we can find the resonant frequency as:

$$fo = \frac{nc}{2\pi r\sqrt{\varepsilon eff}} \quad (3)$$

Where
r: the main radius of the ring element
λ_g: the guided wave length
n: the mode number, 1, 2, 3, ...
f_o: the resonant frequency
$\varepsilon_{eff:}$ the effective of dielectric constant
C: the speed of the light (3 x 10^8)

For the 50 Ω characteristic impedance Zo, the w/d ratio can be found using this formula:

$$\frac{w}{d} = \frac{8e^A}{e^{2A}-2} \quad (4)$$

For w/d < 2

$$\varepsilon e = \frac{\epsilon r-1}{2} + \frac{\epsilon r-1}{2}\frac{1}{\sqrt{1+\frac{12d}{w}}} \quad (5)$$

Where:

$$A = \frac{Zo}{60}\sqrt{\frac{\varepsilon r+1}{2}} + \frac{\epsilon r-1}{\varepsilon r+1}\left(0.23 + \frac{0.11}{\varepsilon r}\right) \quad (6)$$

For the main radius, it can be calculated using this formula:

$$r = \frac{n\lambda g}{2\pi} \quad (7)$$

In this study a 2.2GHz Microstrip ring-resonator is designed on the CST simulation Software. The materials used for this ring resonator are Roger RT/Duriod 5880 substrate with its dielectric constant 2.2 and height of 0.787mm. The total size of the circuit is 100 mm x 68 mm x0.787mm (L x W x H) respectively. All design parameters of the Microstrip ring resonator are listed in Table 1:

Table 1: Microstrip Design Parameters

Parameter	Design Value
Substrate: Roger RT/Duriod 5880	ε= 2.2
Zo	50 Ω
Lg	100 mm
Wg	68 mm
h	0.787 mm
r	15.85 mm
t	0.0175 mm
w	2.5 mm
l	34 mm

Two-Port Ring Resonator

The design structure for the two-port ring resonator; which is illustrated as in figure1, has two coupling gaps. This coupling gap is an important part of the ring resonator and it is separating the feed lines from the ring which allows the structure to only support selective frequencies. The performance of the ring is dependent on the size of the coupling gap. When the used size is very small, a lower loss will occur, but it affects the fields in the resonant structure. On the other words, a larger gap size will

result more losses but less field perturbation.

When standing wave is set up, the resonance occurs in the ring. This happens when its circumference is an integral multiple of the guided wavelength. It is imperative to first understand the ring field configuration for different modes in order to understand its basic phenomena underlying the operation. In the absence of the slits or other discontinuities, a maximum field point occurs where the feed line excites the resonator. This point is independent of the azimuthal position of the feed line that extract microwave power. The absolute values of maximum field point of the first mode for the two-port ring resonators of port 1 and 2 are shown in figure 2.

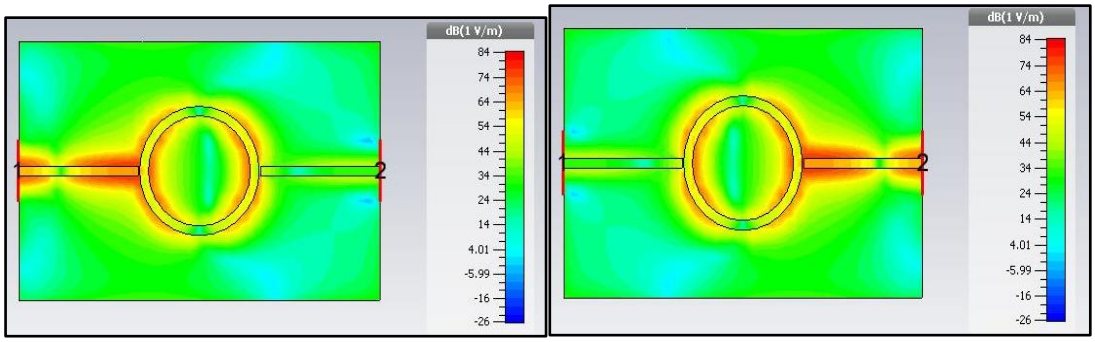

(a) (b)

Figure 2: Absolute values of maximum field point of a): port 1, b): port 2

Ring Resonator with one Slit

The structure design in figure 3 demonstrates the ring resonator with one slit at positive 90 degrees and its maximum fields point at the first resonant mode. The maximum modes that this structure supports are the n = 1.5, 2, 2.5, 3.5, 4..., and so on. In this design the odd modes are not supported, while the half modes are supported in this design structure. The fields in the resonator are altered in the presence of slits so that can corresponding boundary condition is satisfied. Due to this, the maximum field points of some modes are not collinear, but appear skewed about the feed lines.

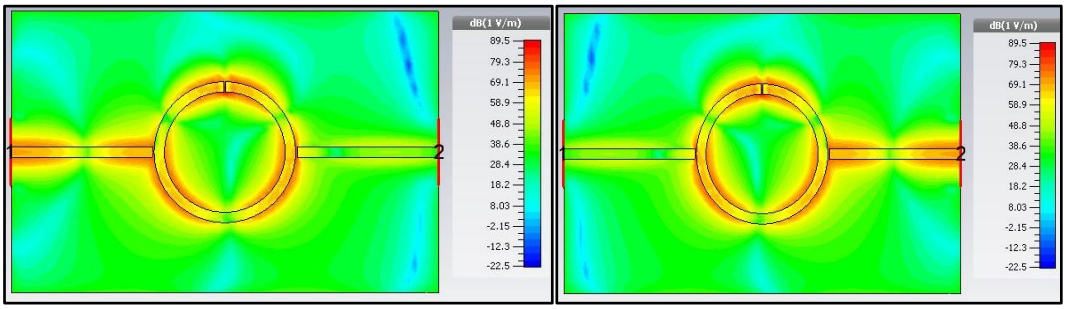

(a)(b)

Figure 3: maximum electric field points for mode n=1.5 for MRR with one slit a): port 1, b): port 2.

Two-Slit Ring Resonator

The maximum filed points is shown figure 4 for the ring resonator design with two slits, which are located at 90 degrees in the positive and negative side of the y- axes. The maximum field points for the first mode supported by this design is at mode n =2. The modes that this structure supports are the n= 2, 4, 6…, and so on. However, all the odd modes are suppressed and there is no half-mode in this structure design.

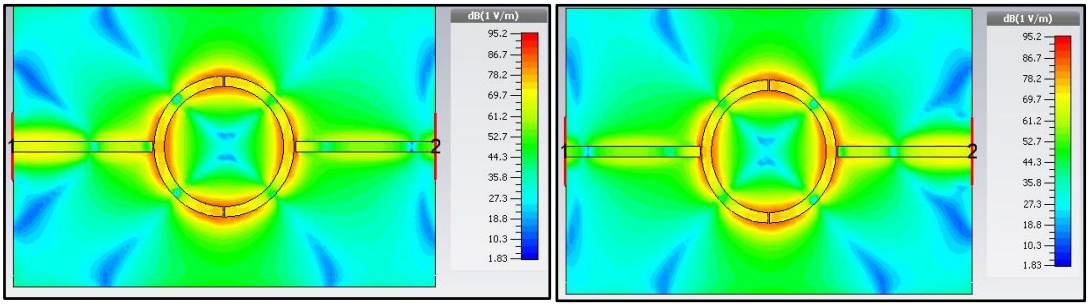

(a)(b)

Figure 4: Maximum field point of MRR with two slits at n =2 a): port 1, b): port 2.

Stub-Matched Loose Coupling Ring Resonator

The coupling efficiency between the Microstrip feed-lines and the annular Microstrip ring element will affect the resonant frequency and Q- factor of the circuit in the two port ring resonator with coupling gap. It also suffers from high insertion loss because of its small effective coupling area. Hence, the design shown in figure 5 is used to increase the coupling energy by using the matched coupling stub.

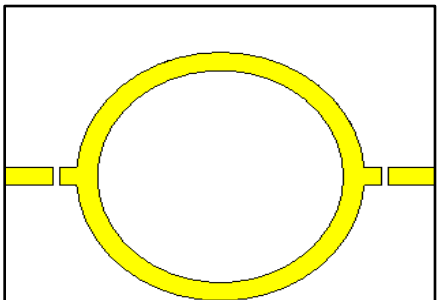

Figure 5: Design structure for stub matched loose coupling

Although the loose- coupling method shown in the two-port ring resonator with coupling gap is the most commonly used among all types of resonators, it suffers from high insertion loss. In order to improve the high insertion loss caused by loose couplings, an enhanced coupling ring is used and the reason for using this design is to increase the coupling strength between the feed line and the ring resonators. By increasing the coupling periphery (at angle points 0^o and 180^o), the insertion loss of the ring can be reduced with a minimal field perturbation.

Enhanced-Coupling Ring Resonator

The design structure for enhancing coupling ring resonator is shown in figure 6. To double the coupling periphery compared to two-port gap coupling in this design, two gaps were introduced in the ring with the feedlines extending in between these gaps. Here it is important to ensure that physical lengths of the two halves of the resonator are identical to avoid mode splitting. This design structure is particularly attractive for optoelectronic application that requires splitting of the resonator to facility DC biasing.

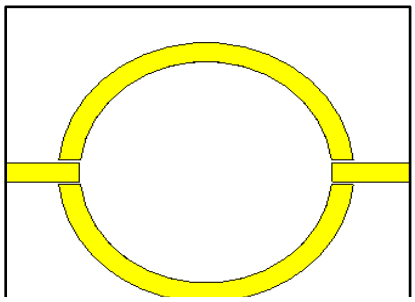

Figure 6: Design structure of enhanced coupling ring resonator

Results and Discussions

The Ring resonator was designed using the CST software simulator and the simulated result is shown in figure 7 for unloaded condition resonator. It illustrates a periodic resonance at 2.2GHz interval when simulating the first resonance mode at 2.13GHz and the second is at 4.1GHz and then third at 6.3GHz and the last resonance which is occurred at 8.3GHz. Since using the loose coupling to the ring resonator, the result of S21 is seemed lossy.

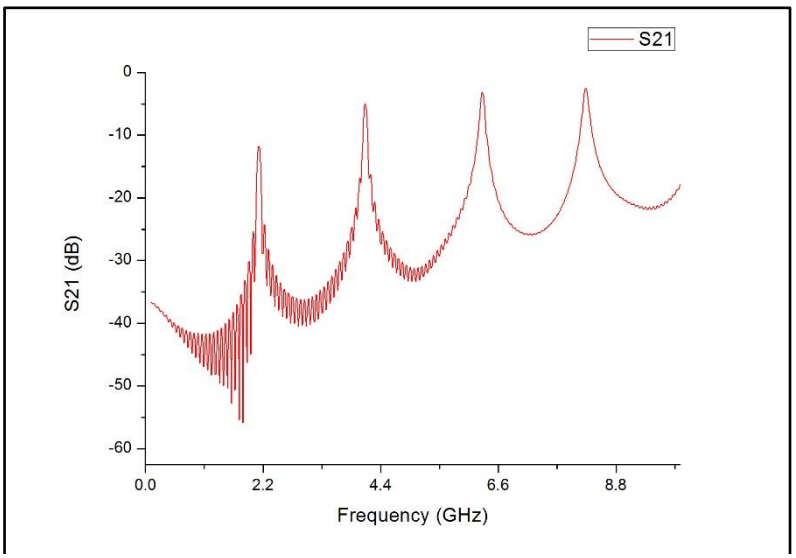

Figure 7: S_{21} parameters of Two-Port Ring Resonator with unloaded material

The simulated result is shown in Figure 8 which is demonstrating the ring resonator with one slit at 90^{o}. As can be seen, the first resonant peak occurs approximately at 3.14 GHz, which is corresponds to the half-mode n=1.5 as the theoretical result in Table 2. The even mode is centered between the half-modes of peak resonant frequency of 4.17GHz, which corresponds to n=2. The half-modes at point n=1.5 and n=2.5; which are corresponding to the resonant frequency of 3.14GHz and 5.27GHz respectively, are approximately 10dB down when compared to the even mode at 4.17GHz resonant frequency of point n=2.

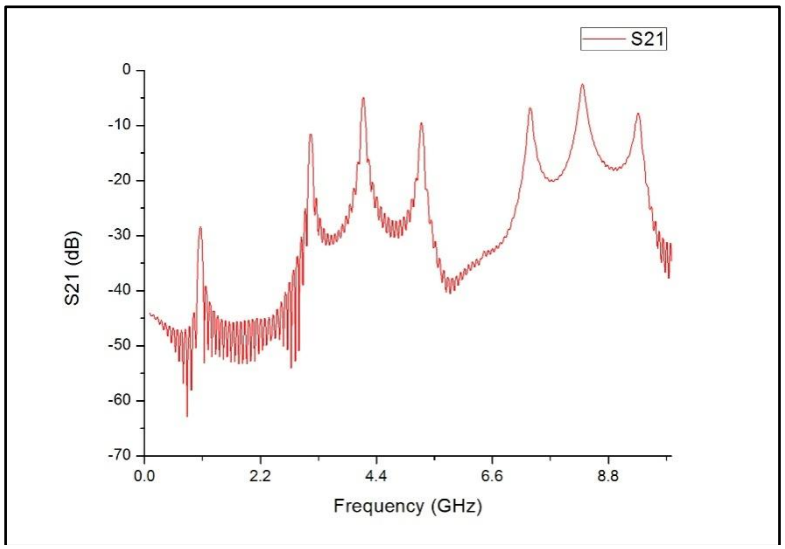

Figure 8: S21 parameters of MRR with one slit

Table 2: Theoretical and measured frequency at different modes for MRR with one slit

Modes (n)	One-Slit			
	Calculated f_r (GHz)	Measured f_r (GHz)	S21 (dB)	S11 (dB)
1.5	3.299	3.14	-11.96	-2.87
2	4.399	4.17	-5.28	-7.61
2.5	5.499	5.27	-9.96	-4.18
3.5	7.699	7.34	-7.32	-5.87
4	8.799	8.29	-3.32	-13.94
4.5	9.899	9.38	-8.17	-5.36

In Figure 9, the even modes, n=2, 4, 6…, and so on, are supported in this structure of the basic ring resonator. There are no half-modes and all the odd modes are suppressed. The first resonant occurs at approximately 4.16 GHz (n=2) and the second is at 8.29 GHz (n=4), and so on as indicated in Table 3.

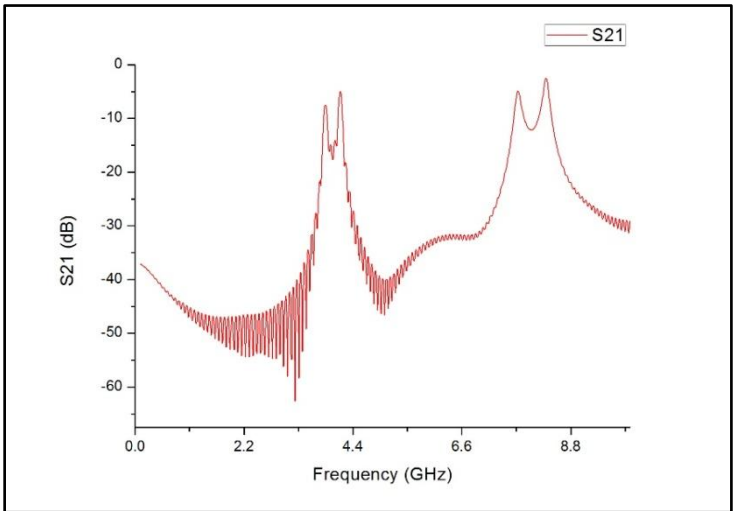

Figure 9:S21 parameters for MRR with two-slit

Table 3: Theoretical and measured frequency at different modes for MRR with one slit

Modes (n)	Two-Slit			
	Calculated f_r (GHz)	Measured f_r (GHz)	S21 (dB)	S11 (dB)
2	4.399	4.16	-5.26	-7.71
4	8.799	8.32	-2.69	-13.69

A comparison between the resonance frequencies and insertion losses of the first four modes of the proposed designs is shown in table 4. The resonance frequencies are marginally different due to the variation of the coupling capacitance between the feed line and the resonator. The insertion loss is reduced when using a stub matched loose coupling instead of the two coupling gaps between the feed line and resonator as shown in figure 9, 10. It is employed to lower the insertion loss in line with the suitable application. When using an enhanced-coupling, the return loss is better from the result of the basic design for coupling gaps ring resonator as well as the insertion loss that is indicated in Table 5.

Table 4: Comparison of resonance frequencies and insertion losses of the first four modes with different excitation designs

Mode (n)	Two-Port			Stub-Matched			Enhanced-Coupling		
	Calculated f_r (GHz)	Measured f_r (GHz)	S21 (dB)	Calculated f_r (GHz)	Measured f_r (GHz)	S21 (dB)	Calculated f_r (GHz)	Measured f_r (GHz)	S21 (dB)
1	2.199	2.13	-11.89	2.199	2.03	-13.52	2.199	2.19	-6.24
2	4.399	4.1	-5.23	4.399	3.94	-5.82	4.399	4.30	-1.77
3	6.599	6.3	-3.30	6.599	6.01	-3.18	6.599	6.59	-1.26
4	8.799	8.3	-2.60	8.799	7.88	-2.08	8.799	8.63	-1.28

Table 5: Comparison of resonance frequencies and return loss of the first four modes with different excitation designs

Mode (n)	Two-Port			Stub-Matched			Enhanced-Coupling		
	Calculated f_r (GHz)	Measured f_r (GHz)	S11 (dB)	Calculated f_r (GHz)	Measured f_r (GHz)	S11 (dB)	Calculated f_r (GHz)	Measured f_r (GHz)	S11 (dB)
1	2.199	2.13	-2.74	2.199	2.03	-2.21	2.199	2.19	-6.49
2	4.399	4.1	-7.43	4.399	3.94	-7.01	4.399	4.30	-15.94
3	6.599	6.3	-11.99	6.599	6.01	-13.73	6.599	6.59	-20.02
4	8.799	8.3	-13.23	8.799	7.88	-17.99	8.799	8.63	-21.32

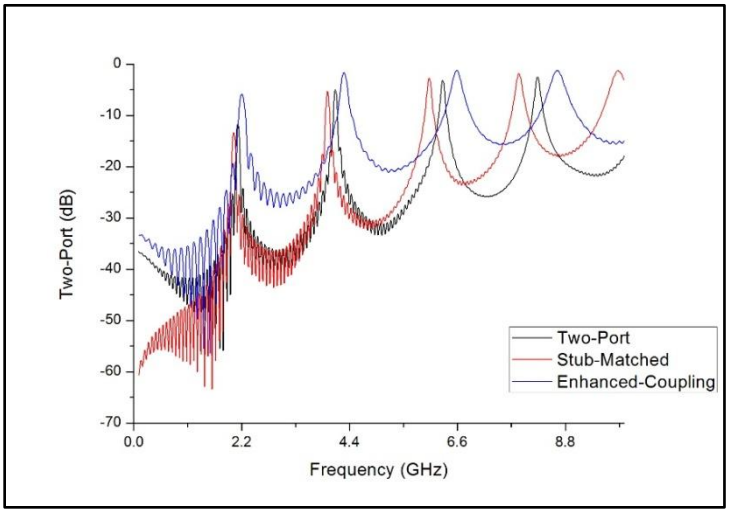

Figure 9: comparison of resonance frequencies for insertion loss at different excitation designs

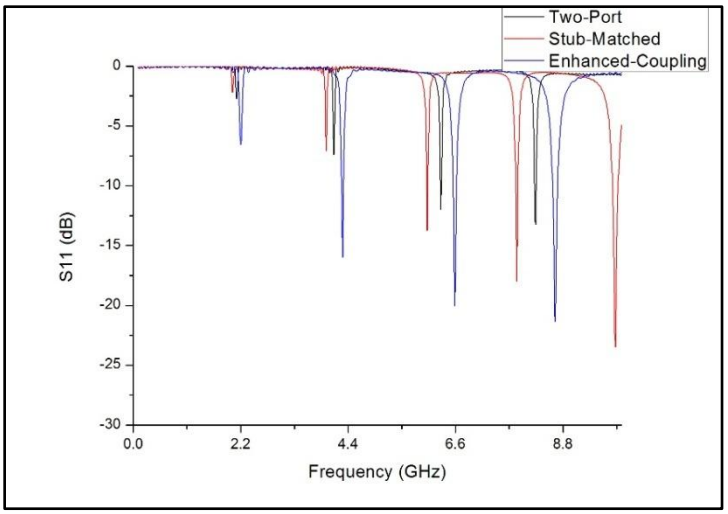

Figure 10: comparison of resonance frequencies for insertion loss at different excitation designs

Conclusion

For determining the dielectric constant of a low loss dielectric materials, unloaded microwave ring resonator with coupling gaps is examined in details and reviewed different techniques for its analysis. An enhanced coupled ring resonator for lower insertion loss is proposed and demonstrated. These designs does not alter the functionality of the ring, but they are minimally perturbing. The enhancement designs exhibit the lowest insertion loss, and in each case further improvements are possible by decreasing the size of the coupling gap. This feature is expected to be particularly useful for bio-sensing and characterizing materials of liquids and solids. The proposed ring resonatorshave simple structure, easy fabrication and does not require time consuming for processing.

Acknowledgment

This work is supported by UTeM and funded by the Malaysian Government under research grants RAGS/1/2014/TK03/UTEM//14.

References

[1] Khir, M.S. and Hammad, H.F., 2002, “Measurement of the Dielectric Constant of Liquid using a Hybrid Cavity Ring resonator”, PIERS Proceedings, Cambridge, USA.

[2] Sheen, J., 2007, “Amendment of Cavity Perturbation Technique for Loss Tangent Measurement at Microwave Frequencies”, J.Appl.Phys. 102.

[3] Sheen, J., 2009, “Measurements of Microwave Dielectric Properties by an Amended Cavity Perturbation Techniques”, Measurement, Vol. 42, pp. 57- 61.

[4] Yong, H.K., Sheung, Y., Park, S.C., Lim, D.H., Jung, H.I., Kim, and Y.J., 2008, “A Simple and Direct Biomolecules Detection Scheme Based on a Microwave Resonator”, Sensors and Actuators B Vol. 130, pp. 823-828.

[5] Samanta, K.K., Stephens, D., and Robertson, I.D., 2005, ‘Ultra-wideband characterization of photo-imageable thick film materials for microwave and millimeter-wave design’, Microwave Symp. Digest, IEEE MTT-S Int.

[6] Thompson, D.C., Tantot, O., Jallageas, H., Ponchak, G.E., Tentzeris, M.M., and Papapolymerou, J., 2004, ‘Characterization of liquid crystal polymer (LCP) material and transmission lines on LCP substrates from 30 to 110 GHz’, IEEE Trans. Microw. Theory Tech.

[7] Gardner, P., Paul D. K., and Tan, K. P., 1994, "Planar Microstrip Ring Resonator Filters" Department of Electrical Engineering and Electronics.

[8] Sheng, S., and Lei, Z., 2007, "Wideband Microstrip Ring Resonator Band-pass Filters under Multiple Resonances" IEEE Trans. Microwave Theory Tech, vol.55.

[9] Kunnthphong, S., Apisak, W., and Wanlop, S., 2010, "Design of Triple-Mode Ring Resonator for Wideband Microstrip Band-pass Filters" IEEE Trans. Microwave Theory Tech, vol.55.

[10] Pozar, D. M., 1990, “Microwave engineering”, Addison-Wesley Publishing Company.
[11] Chang, 1996, “Microwave ring circuits and Antennas”, John Wiley & Sons.
[12] Jilani, M. T., Wen, W. P., Zakariya, M. A., and Cheong, L. Y., 2013, "Microstrip Ring Resonator Based Sensing Technique for Meat Quality", IEEE Symposium on Wireless Technology and Applications (ISWTA).
[13] JLANI, M. T., WEN, W. P., and ET AL., 2014, "Equivalent Circuit Modeling of the Dielectric Loaded Microwave Biosensor", Radio-engineering, VOL. 23, NO. 4.
[14] Aoyagi, S., and Kudo, M., 2005, “Observation of fluorescencelabeled protein A on a biosensor surface by means of TOF-SIMS, ” Sens. Actuator B-Chem., 108, 708-712.
[15] Fritz, J., Baller, M. K., Lang, H. P., Rothuizen, H., Vettiger, P., Meyer, E., Guntherodt, H.-J., Gerber, Ch., andGimzewski, J. K., 2000, “Translating Biomelecular Recognition into Nanomechanics, ” Science, 288, 316-318.
[16] Guan, W.-J., Li, Y., Chen, Y.-Q., Zhang, X.-B., and Hu, X.-B., 2005, “Glucose biosensor based on multi-wall carbon nanotubes an screen printed carbon electrodes, ” Biosens.Bioeletron., 21, 508-512.
[17] Dostalek, J., Vaisocherova, H., and Hmola, J., 2005, “Multichannel surface plasmon resonance biosensor with wavelength division multiplexing, ” Sens. Actuator B-Chem., 108, 758-764.